Correlation for Photocatalytic Degradation Kinetics of Carboxylic Acids using Electrochemically Synthesized Al₂S₃ Nanoparticles and Study of Antibacterial Activity

H.C. Charan Kumar, R. Shilpa and Sannaiah Ananda[*]

Department of Studies in Chemistry, University of Mysore, Mysore-570006, India

*Corresponding author: E-mail: snananda@yahoo.com

Aluminium sulfide (Al₂S₃) nanoparticles were successfully synthesized by electrochemical method. Further, the synthesized nanoparticles were used as a photocatalyst for degradation of trichloroacetic acid, chloroacetic acid, acetic acid and degradation kinetics was studied by volumetric method using NaOH under various experimental conditions. The Al₂S₃ nanoparticles were characterized by UV-visible spectroscopy, X-ray diffraction and SEM-EDAX. The study of UV-visible spectroscopy indicates that Al₂S₃ nanoparticles shows maximum intensity peak at 222 nm in the UV region and there is no absorption peak in the visible region, therefore the synthesized nanoparticles is active under UV light and band gap energy was found to be 3.07 eV, which was calculated using Tauc plot. The structure of Al₂S₃ was found to be tetragonal structure and average crystal size was found to be 25.76 nm, which was calculated using Debye-Scherrer's formula. The SEM results showed that Al₂S₃ appears as nanoflakes with agglomerated. The presence of aluminium and sulfur was confirmed using EDAX spectra. The photocatalytic activity of the synthesized Al₂S₃ nanoparticles was examined by taking three carboxylic acids by volumetric method. Taft LFER was tested, the isokinetic temperature β was calculated for oxidation of carboxylic acids. The antibacterial activity was investigated for synthesized nanoparticles by using *Bacillus subtilis* MTCC 2763 and *Escherichia coli* MTCC 40 of different bacteria.

Keywords: Electrochemical method, Aluminium sulfide nanoparticles, Carboxylic acids, Antibacterial activity.

INTRODUCTION

In recent years, the study of nanoscience is a broad area of research and development activity that has been growing explosively for many researchers. Aluminium sulfide (Al₂S₃) nanoparticles show a good applications in many areas of research compare to Al₂O₃ nanoparticles especially in opto-electronic, solar cells, transparent electrodes, phototransistors, gas sensors and photodiodes [1,2]. Catalysis using Al₂S₃ nanoparticles is a subject of great interest and intensive research is being carried out to ensure the biological applications [3-5]. Al₂S₃ Nanoparticles has widely explored as a bifunctional catalyst for oxygen reduction reactions and oxygen evolution reactions (OER), due to their good physical and chemical properties [6-8]. In broad range of devices Al₂S₃ has been incoordinate along with heterogeneous catalysts energy storage devices and energy conversion. Many of these functions enforced numerous coating and thin film coatings technique [9-11].

Nanosized Al₂S₃ in photocatalysts were consideration as an encouraging tool for appliance in the purification of waste-water and hydrogen energy production [12-14]. Al₂S₃ is a colour-less solid with a variety of crystalline structures and sensitive to moisture and hydrolyzes readily in contact with water and slowly in moist air, generating gaseous H₂S [15-18]. Many researchers [19-23] reported the incorporation of semicond-uctor Al₂S₃ nanomaterials into polymers by chemical methods. In the present study, Al₂S₃ nanoparticles were synthesized by electrochemical method, which is an environmentally friendly method. The synthesized Al₂S₃ nanoparticles were used as a photocatalyst for the degradation of carboxylic acids (tri-chloroacetic acid, chloroacetic acid, acetic acid) and its degraded kinetics were studied by volumetric method using NaOH solution.

EXPERIMENTAL

All chemicals used to prepare Al₂S₃ nanoparticles were analytical grades of purity. Aluminium electrode was purchased

from Alfa Aesar. Trichloroacetic acid, chloroacetic acid and acetic acid from Lobachemie, platinum electrode from Elico Pvt. Ltd. All solutions were prepared in double-distilled water. The optical properties for prepared aluminium sulfide nanoparticles were studied by UV-visible spectrophotometer (Shimadzu-1700 series). The X-ray crystallographic interpretations were performed by X-ray diffractometer (panalytical x-pert) using CuKα wavelength (λ = 1.54 Å) scanning range from 0 to 70 Å. The morphological feature for the prepared aluminium sulfide study was determined by scanning electron microscopy (SEM-EDEX) from Quanta-200 FEI, Netherlands. The elemental analysis for the conformation of prepared Al and S is confirmed from energy dispersive X-ray analysis (EDAX).

Synthesis of Al$_2$S$_3$ nanoparticles by electrochemical method: Al$_2$S$_3$ Nanoparticles were synthesized by electrochemical method by using Al electrode in an aqueous system with Na$_2$S as a conductive salt. The Na$_2$S acts as the sulphur source. The two electrodes were dipped in the Na$_2$S solution and connected to the poles of a battery. The Al metal electrode was connected to the positive terminal as anode and platinum electrode was connected to a negative terminal called cathode, using 20 mA current and potential of 10 V the experiment was run for 2 h with continues stirring. The electrolytic cell is consisting of 0.2 M of Na$_2$S solution. The distance of the anode and cathode during electrolysis was 2 cm. The electrochemically generated S^{2-} species reacted with Al^{3+} in the electrolyte to produce Al$_2$S$_3$ nanoparticles. The experimental set up as shown in Fig. 1 during electrolysis Al electrode get oxidized to give Al^{3+} and react with S^{2-} species to give Al$_2$S$_3$ nanoparticles. The obtained solid is washed with double distilled water till complete removal of unreacted Na$_2$S. The solid Al$_2$S$_3$ was centrifuged and calcined for 2 h at 800 ºC for dehydration and for the removal of sodium hydroxide impurities, which has formed in electrolysis and atmospheric oxidation. The mechanism for the synthesized Al$_2$S$_3$ nanomaterial is given in **Scheme-I**.

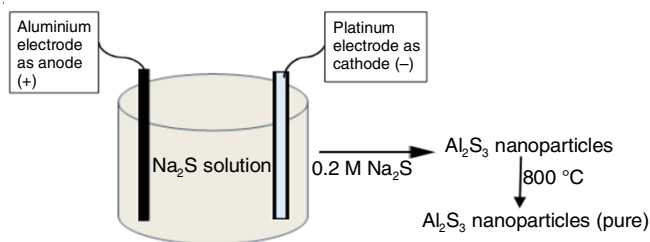Fig. 1. Experimental set up for the electrochemical synthesis of Al$_2$S$_3$ nanoparticles

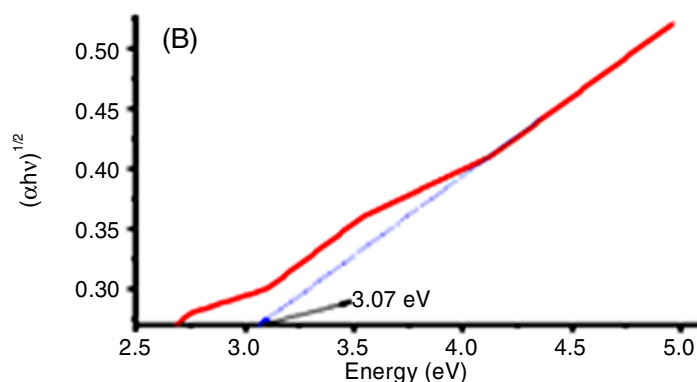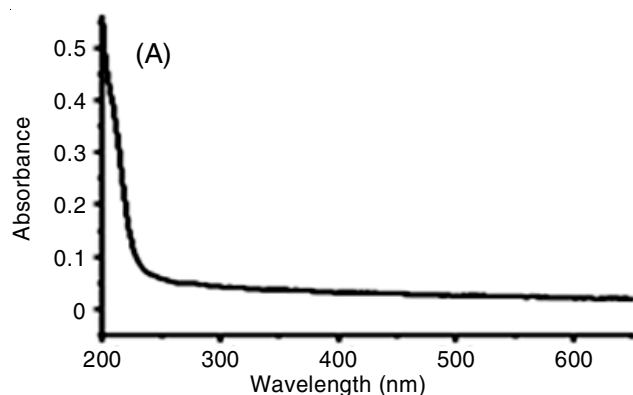$$Al \rightleftharpoons Al^{3+} + 3e^-$$
$$Na_2S + 2H_2O \rightleftharpoons 2NaOH + S^{2-} + H_2$$
$$2Al^{3+} + 3S^{2-} \rightleftharpoons Al_2S_3$$
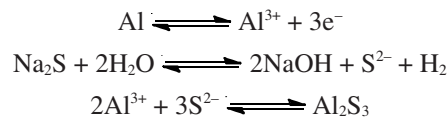
Scheme-I

Determination of photodegradation kinetics by volumetric method: In the present work, the volumetric titration method was used to determine the degradation efficiency, by measuring the concentration of carboxylic acid by the titration against NaOH solution at different time intervals. The different concentration of acid solutions (0.5×10^{-3} to 3×10^{-3} M) were prepared using double distilled water. This solution was used as a test contaminant for evaluating photocatalytic activities of the prepared Al$_2$S$_3$ nanoparticles. The experiment was carried out under tungsten-halogen UV-light in order to check the effect of Al$_2$S$_3$ nanoparticles. After the complete degradation of carboxylic acid no colour formation takes place with phenophthaline-NaOH solution. A plot of log V/V$_o$ *versus* time was linear up to 60% of the reaction illustrates the appearance of carboxylic acid follows first order kinetics. The COD values had been investigated for both before and after degradation of all the carboxylic acid solutions using dichromate oxidation method [24,25]. The COD values were calculated by the following eqn.:

$$COD = \frac{(Blank - Sample) \times N_{FAS}}{V_{Sample}} \times 8000$$

RESULTS AND DISCUSSION

UV-visible analysis: It is confirmed that from the optical absorption spectra that the absorption band of Al$_2$S$_3$ nanoparticles showed a blue shift, which is due to particle size in the nano region [26,27]. Fig. 2 shows that the synthesized Al$_2$S$_3$ nanoparticles has maximum intensity peak at 222 nm in the UV-region and there is no absorption peak in the visible region. Further, the rate of degradation of carboxylic acids in presence of sunlight is very slow as compared to UV light. The UV-visible spectrum of Al$_2$S$_3$ nanoparticles over the range 200-700 nm showed that the synthesized nanoparticles were photoactive under ultraviolet radiation. The band gap of synthesized Al$_2$S$_3$ nanoparticles was calculated using Tauc's plot [28,29] by plotting (αhν)$^{1/2}$ *versus* hν. The band gap energy of Al$_2$S$_3$ nanoparticle was found to be 3.07 eV.

Fig. 2. UV-visible spectra (A) and Tauc plot (B) of Al$_2$S$_3$ nanoparticles

XRD analysis: Fig. 3 shows the XRD pattern of synthesized Al₂S₃ nanoparticles. The obtained peaks indicates the presence of mixed phases of Al₂S₃. The position of the peak appearing at 2θ values was 37.33º, 45.74º, 66.81º can be readily indexed as (111), (212), (204) crystal planes of Al₂S₃ nanoparticles. All these diffraction peaks can be perfectly matched with respect to their position with tetragonal crystal structure. Debye-Scherrer's equation $[D = k\lambda/\beta\cos\theta]$ was employed to calculate average crystallite size of the synthesized Al₂S₃
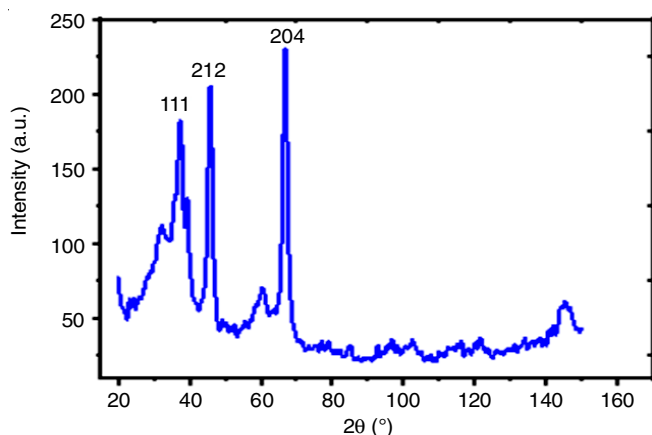
nanoparticles and found to be 25.76 nm [25]. Hence, XRD analysis clearly indicates the presence of Al₂S₃ nano composition.

SEM analysis: Fig. 4 indicates that Al₂S₃ nanoparticles were spherical structure and shows nanoflakes when observed at different magnification. It is also clear that the particles were agglomerated in nature. The SEM image shows randomly distrubuted Al₂S₃ grains with smaller size. The EDAX spectrum confirmed the presence of Al and S in the nanomaterial.

Photodegradation kinetics and COD measurements

Effect of carboxylic acids concentration: The effects of concentration of carboxylic acids on the photodegradation were carried out at four different concentrations of carboxylic acid solutions varying from 0.5×10^{-3} to 3×10^{-3} M at constant weight of Al₂S₃ nanoparticles. The change in concentration of the carboxylic acids was recorded by appearance of pink colour by using NaOH solution by volumetric method. A plot of log V/V₀ *versus* time was linear up to 60% of the reaction illustrate the disappearance of carboxylic acid follows first order kinetics (Fig. 5). The rate constant values are given in Table-1 and the rate of reaction decreased with increase the acid solution. The reason beyond with increase the acid concentration, the solution becomes more intense and the path-length of photons increase entering the solution and the rate of reaction is decreased and

Fig. 3. XRD pattern of Al₂S₃ nanoparticles
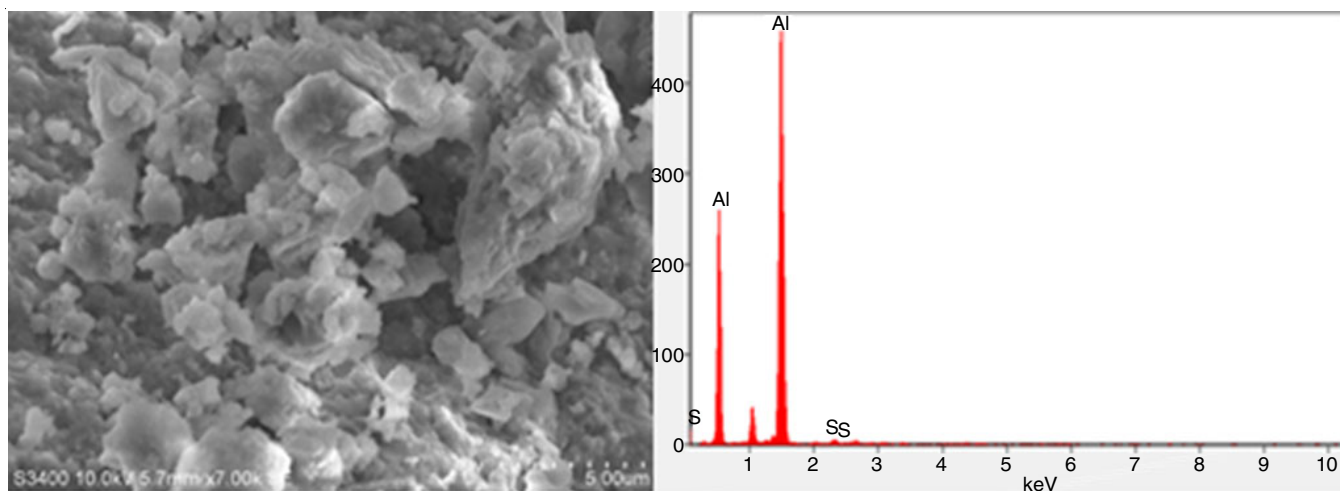

Fig. 4. SEM and EDAX images of electrochemically synthesized Al₂S₃ nanoparticles
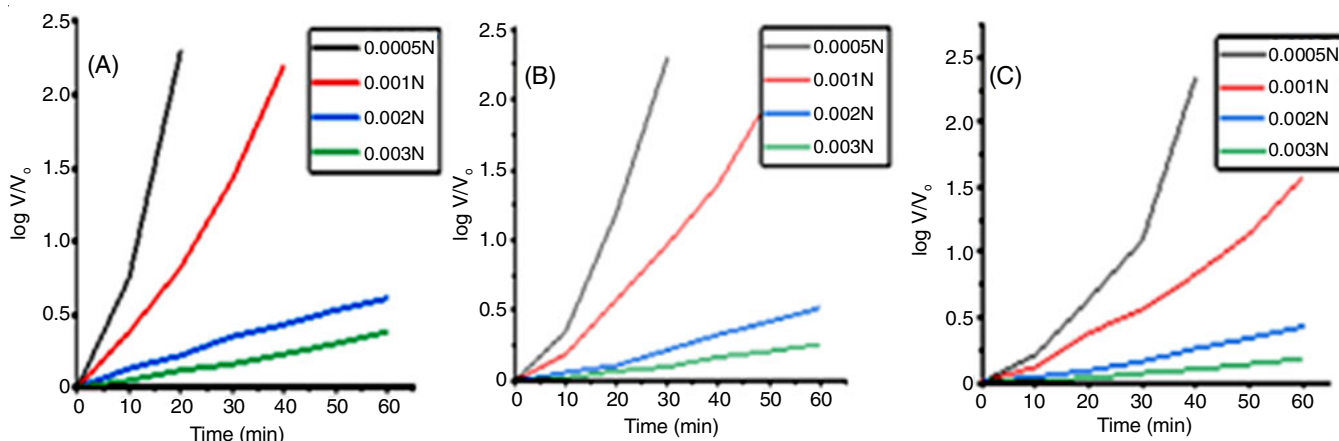

Fig. 5. Effect of concentration of carboxylic acids on the rate of degradation under UV light (A) trichloroacetic acid (B) chloroacetic acid (C) acetic acid
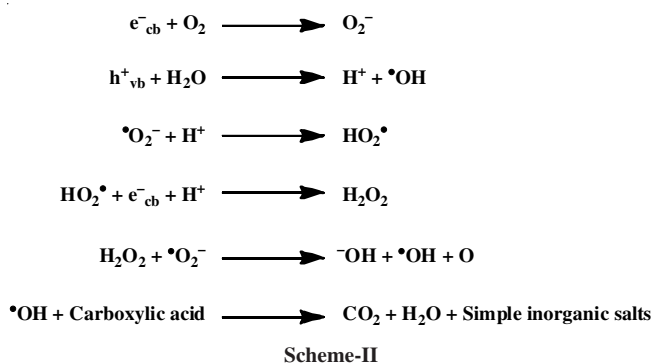
TABLE-1
EFFECT OF PHOTODEGRADATION AT DIFFERENT CONCENTRATION OF CARBOXYLIC ACIDS UNDER UV LIGHT

Catalyst (0.02 g)	Carboxylic acid	Concentration of acid in 10^{-3} N	10^{-3} (k s^{-1})	Time taken for 95% degradation (min)	COD Values (mg/L)		Photodegradation efficiency (%)
					Before degradation	After degradation	
Al$_2$S$_3$ nanoparticles	Cl$_3$CCOOH	0.5	4.41	15	512	8	98.43
		1.0	2.08	50	992	16	98.38
		2.0	0.38	230	1216	16	98.68
		3.0	0.24	380	1296	32	97.53
	ClCH$_2$COOH	0.5	2.97	30	416	16	96.15
		1.0	1.89	60	704	16	97.72
		2.0	0.34	270	816	32	96.07
		3.0	0.17	390	992	32	96.77
	CH$_3$COOH	0.5	2.14	50	352	16	95.45
		1.0	0.99	90	544	16	97.05
		2.0	0.28	290	592	32	94.59
		3.0	0.11	410	672	32	95.23

a few photons reached the catalyst surface. Hence, the productions of hydroxyl radicals were reduced. Therefore, the photodegradation efficiency is reduced.

The COD were measured before and after degradation and are given in Table-1. To account for the mineralization of acids solution, COD value was also investigated at different stages (Fig. 6). The formation of different radical species during photodegradation is given in **Scheme-II**. The carboxylic acid solution was found to have mineralized into H$_2$O, CO$_2$ and inorganic salts [30]. The photodegradation efficiency of the photocatalyst was calculated by the following eqn.:

$$\text{Photodegradation efficiency} = \frac{\text{Initial COD} - \text{Final COD}}{\text{Initial COD}} \times 100$$

$$e^-_{cb} + O_2 \longrightarrow O_2^-$$

$$h^+_{vb} + H_2O \longrightarrow H^+ + {}^\bullet OH$$

$${}^\bullet O_2^- + H^+ \longrightarrow HO_2^\bullet$$

$$HO_2^\bullet + e^-_{cb} + H^+ \longrightarrow H_2O_2$$

$$H_2O_2 + {}^\bullet O_2^- \longrightarrow {}^- OH + {}^\bullet OH + O$$

$${}^\bullet OH + \text{Carboxylic acid} \longrightarrow CO_2 + H_2O + \text{Simple inorganic salts}$$

Scheme-II

Effect of catalyst loading: Effect of catalyst was carried out by taking four different amount of catalyst varying from 0.005 to 0.03 g keeping acid concentration constant. The study showed that the increase of the catalyst from 0.005 to 0.03 g increased degradation efficiency of acid. Further with increase of catalyst above 0.02 g photoactivity of catalyst is decreased, due to aggregation of Al$_2$S$_3$ nanoparticles at higher concentration causing a decrease in the number of active sites on catalyst surface and increase in the light scattering of Al$_2$S$_3$ nanoparticles [31]. This tends to decrease the passage of light through the sample. Further, the present study indicated, the optimized photocatalyst loading is 0.02 g/20 mL. The rate constant and COD values are reported in Table-2 and Figs. 7 & 8.

Effect of temperature: It was observed that when temperature increased, the degradation efficiency of acid is increased, and the rate of degradation is not very significant at low temperature. However, the reaction is more significantly influenced at high temperature since the diffusion rate increased with temperature. An increase of temperature could bring about an increase in the degradation rate [32]. The rate constant and COD values are given in Table-3 and Figs. 9 and 10. The Thermodynamic parameters were calculated for carboxylic acids degradation and are reported in Table-4.

Linear free energy relation (LFER): The structural modification of a reactant molecule may influence the rate or equilibrium constant of a reaction through polar, steric and resonance effects. Out of a number of empirical models for the description of relationships between structures and reactivity the most successful and intensively used are the linear free energy relationships. The experiment were made to arrive at a linear free energy
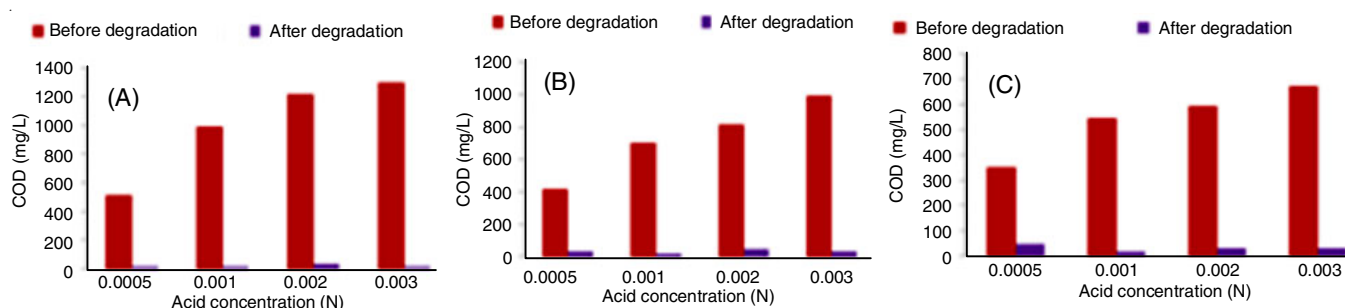

Fig. 6. Effect of concentration of carboxylic acid on COD values under UV light (A) trichloroacetic acid (B) chloroacetic acid (C) acetic acid

TABLE-2
EFFECT OF CATALYST LOADING ON THE PHOTODEGRADATION OF CARBOXYLIC ACIDS UNDER UV LIGHT

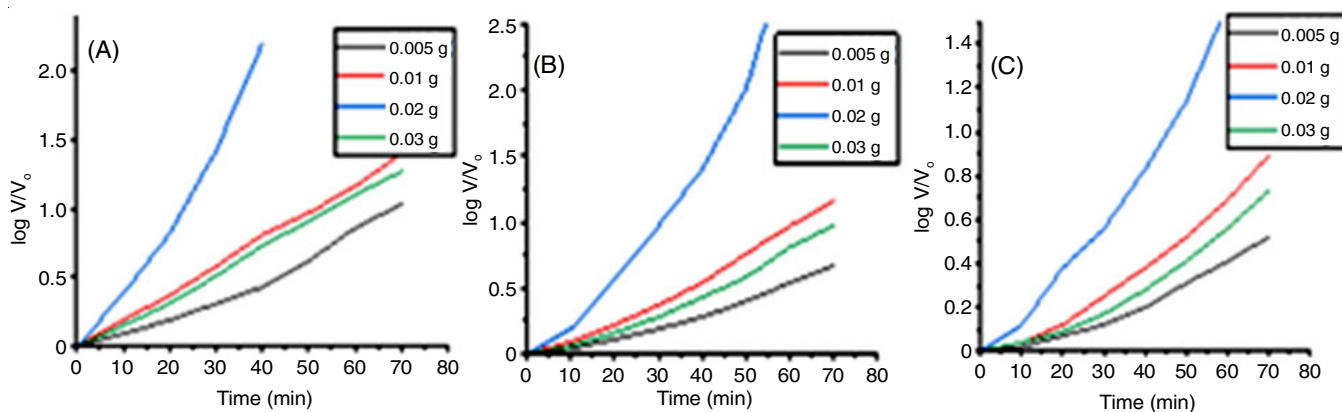| Carboxylic acid	Al$_2$S$_3$ nanoparticles (g)	10^{-3} (k s^{-1})	Time taken for 95% degradation (min)	COD values (mg/L)		Photodegradation efficiency (%)
				Before degradation	After degradation	
Cl$_3$CCOOH (1.0 × 10^{-3} N)	0.005	0.56	180	992	16	98.38
	0.01	0.76	120	992	48	95.16
	0.02	2.08	50	992	16	98.38
	0.03	0.71	60	992	16	98.38
ClCH$_2$COOH (1.0 × 10^{-3} N)	0.005	0.37	240	704	16	97.72
	0.01	0.65	140	704	32	95.23
	0.02	1.89	60	704	16	97.72
	0.03	0.54	80	704	16	97.72
CH$_3$COOH (1.0 × 10^{-3} N)	0.005	0.29	270	544	32	94.11
	0.01	0.49	130	544	16	97.05
	0.02	0.99	90	544	16	97.05
	0.03	0.40	110	544	32	94.11

Fig. 7. Effect of catalyst loading on the rate of degradation of carboxylic acids under UV light (A) trichloroacetic acid (B) chloroacetic acid (C) acetic acid
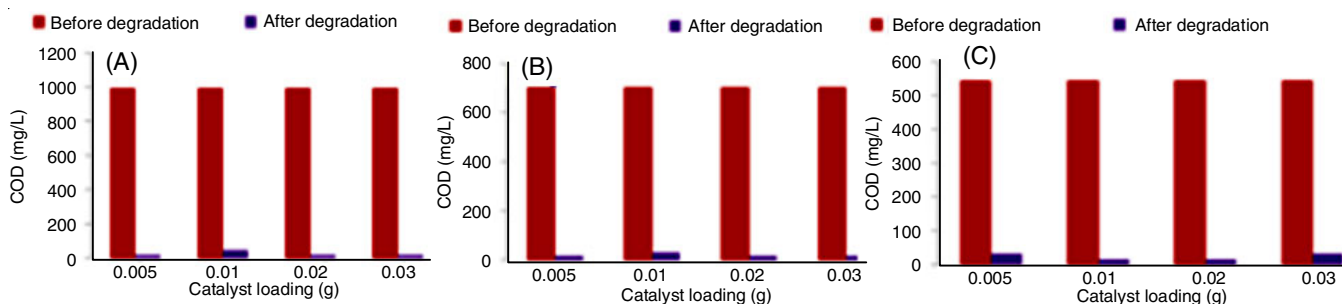

Fig. 8. Effect of catalyst loading of carboxylic acids on COD values under UV light (A) trichloroacetic acid (B) chloroacetic acid (C) acetic acid

TABLE-3
EFFECT OF TEMPERATURE ON THE PHOTODEGRADATION OF CARBOXYLIC ACIDS UNDER UV LIGHT

| Carboxylic acid	Catalyst	Temperature (K)	10^{-3} (k s^{-1})	COD values (mg/L)		Photodegradation efficiency (%)
				Before degradation	After degradation	
Cl$_3$CCOOH (1.0 × 10^{-3} N)	0.02 g Al$_2$S$_3$ nanoparticles	293	0.74	992	16	97.99
		298	2.08	992	16	97.99
		308	2.99	992	32	96.77
ClCH$_2$COOH (1.0 × 10^{-3} N)	0.02 g Al$_3$S$_3$ nanoparticles	293	0.56	704	48	93.18
		298	1.89	704	16	97.72
		308	2.29	704	32	95.45
CH$_3$COOH (1.0 × 10^{-3} N)	0.02 g Al$_2$S$_3$ nanoparticles	293	0.43	544	16	97.05
		298	0.99	544	16	97.05
		308	1.68	544	32	94.11
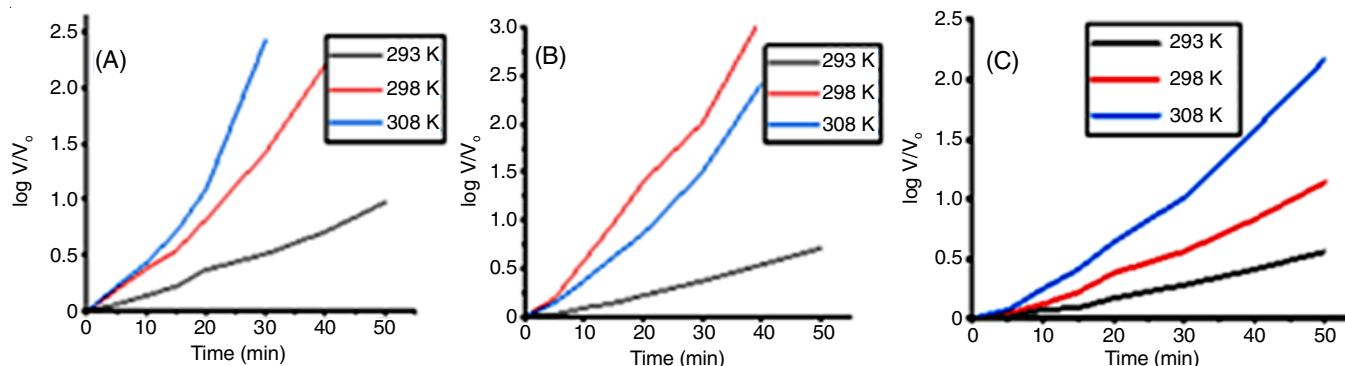
Fig. 9. Effect of temperature on the rate of degradation of carboxylic acids under UV light (A) trichloroacetic acid (B) chloroacetic acid (C) acetic acid
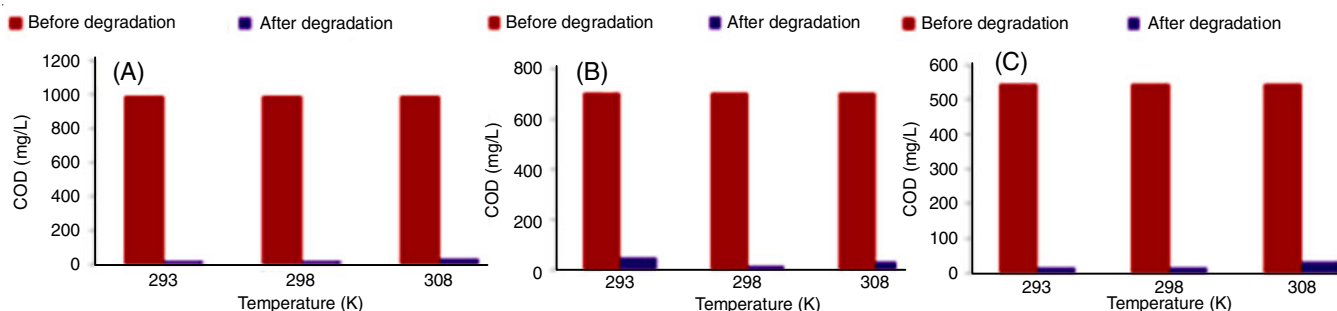

Fig. 10. Effect of temperature of carboxylic acids on COD values under UV light (A) trichloroacetic acid (B) chloroacetic acid (C) acetic acid

TABLE-4
THERMODYNAMIC PARAMETERS FOR CARBOXYLIC ACIDS

Carboxylic acid	Temperature (K)	$\Delta H^{\#}$ (KJ mol^{-1})	$\Delta S^{\#}$ (J K^{-1} mol^{-1})	$\Delta G^{\#}$ (KJ mol^{-1})	E_a
Cl$_3$CCOOH	293 298 308	37.33	-165.21	89.32	9.51
ClCH$_2$COOH	293 298 308	58.75	-94.76	89.64	14.64
CH$_3$COOH	293 298 308	67.38	-70.00	90.86	16.70

relation for the oxidation/photodegradation of carboxylic acids by using Al$_2$S$_3$ nanopartricles. The results of Taft equation were obtained from the plot of log k *versus* σ*. The following regression equation was obtained.

$$\log k = 0.28\ \sigma^* - 3.09\ (r = 0.993) \tag{3}$$

The positive value of polar constant σ* although small it indicate that electron donating capacity decreases the rate of degradation. The rate of oxidation/degradation of carboxylic acids by using Al$_2$S$_3$ nanopartricles decrease in the order:

Trichloroacetic acid > Chloroacetic acid > Acetic acid

The activation energy value is highest for the slowest reaction and *vice-versa* indicated that the reaction is enthalpy controlled. The activation enthalpies ($\Delta H^{\#}$) and entropies ($\Delta S^{\#}$) for the degradation of carboxylic acids through oxidation were linearly related. From the slope of the plot of $\Delta H^{\#}$ *versus* $\Delta S^{\#}$ (r = 0.993) the isokinetic temperature (β) was calculated and found to be 338 K. This is further verified by employing the Exner criterion [33,34] with a plot of log k$_1$ at 298 K *versus* log k$_2$ at 308 K

which is linear. From the Exner′s slope, β was calculated by using following expression [35] and found to be 342 K.

$$\beta = \frac{T_2 T_1 (b-1)}{(bT_2 - T_1)} \tag{4}$$

where, k$_1$ and k$_2$ were the rate constants at temperature T$_2$ and T$_1$, respectively and T$_2$ > T$_1$, b is the slope of log k$_2$ against log k$_1$.

The value of β is higher than the temperature range employed in the present work, supporting the fact that the oxidation of carboxylic acids is enthalpy controlled. The fairly high negative values of entropy of activation point towards the formation of fairly rigid activated state. The constancy of $\Delta G^{\#}$ values indicates that carboxylic acids undergo oxidation/degradation *via* an identical mechanism [36].

Effect of light intensity: The photodegradation rate constant is compared with UV light and sunlight. It is perceived that the photodegradation rate constant is increased in UV light compared to sunlight for synthesized Al$_2$S$_3$ nanoparticles. The reason is due to the fact that when a photon interact on a semi-

conductor (Al_2S_3), the energy overtake the band gap energy of the semiconductor. An electron jumps from the valence band to the conduction band leaving a hole in the valence band. The excited state conduction band electrons and valence band hole can recombined and dissipate energy in the form of heat and get trapped into the metastable surface states, respectively with electrons acceptors and donors that happened to be adsorbed on the semiconductor surface. The stored energy is dissipated within a few nanoseconds by recombination in the absence of suitable e^-/h^+ scavengers. If a suitable scavenger is available to trap the electron, then the recombination could be prevented *i.e.* subsequent redox reaction may occur. Therefore, Al_2S_3 nanoparticles act as a good photocatalyst and is active under UV light compared to sunlight. The rate constant for degradation in sunlight is given in Table-5 and Fig. 11. This also supports the observed energy band gap 3.07 eV in the UV-visible spectral study.

Reuseability of catalyst: The reuse of catalyst was investigated to check the efficiency of photodegradation of carboxylic acid solutions. After the complete degradation of acid solution, degraded acid solution was kept outside for 9 h without exposing the UV-light and supernatant liquid sample was decanted. The catalyst was thoroughly washed with double-distilled water and reuse for the photodegradation by taking new acid solutions. The reuse of photocatalyst shown almost same degradation efficiency compared to the fresh sample. Hence, the photocatalyst can be regenerated and reused.

Degradation in sunlight: A comparison of photoactivity with sunlight was carried out .The photocatalytic experiments were carried out by taking 20 mL of 1.0×10^{-3} N carboxylic acid solution and 0.02 g of synthesized Al_2S_3 nanoparticles in 50 mL beaker. All experiments were carried out in an open atmosphere between the times of 9:45 A.M. to 3:00 P.M. in presence of sunlight. It is clear that rate of degradation is very slow in sunlight compare to UV light (Fig. 11). Hence, the

synthesized nanoparticles were active under UV light. The rate constant values are shown in Table-5.

Antibacterial assay: The antibacterial susceptibility of compound was evaluated by using the disc diffusion Kirby-Bauer method in Mueller Hinton agar plate [37,38]. The study was subjected to evaluate the ability of synthesized nanoparticles as antibacterial agent against two bacterial strains was obtained from Microbial Typing Culture Collection (MTCC), Chandigarh, India. Gram-positive *Bacillus subtilis* (MTCC 2763) and Gram-negative *Escherichia coli* (MTCC 40) were cultured as per the protocol prescribed by MTCC. A 20 mL of sterilized and molten Mueller-Hinton Agar media was poured into the sterilized petri plates. The reference bacterial strains were cultured overnight at 37 ℃ in Mueller-Hinton broth and adjusted to a final density of 107 CFU/mL by 0.5 McFarland standards. A 100 μL of the pathogenic bacteria cultures were transferred onto plate and made culture lawn. The comparative stability of discs containing gentamycin was made. Al_2S_3 Nanoparticles were loaded into 6 mm sterile discs and placed on the culture plates and incubated at 37 ℃ for 24 h. The antibacterial activity was evaluated by measuring the diameter of zone of inhibition (ZOI) formed around the disc, the antibacterial efficacy of Al_2S_3 nanoparticles was determined. All assays were performed in triplicates. The results of antibacterial activity of Al_2S_3 nanoparticles are given in Table-6, it can be concluded that synthesized nanoparticles shows an appreciably good inactivation of different strains of bacteria.

TABLE-6
ANTIBACTERIAL EFFECT OF Al_2S_3 NANOPARTICLES BY
ZONE OF INHIBITION (mm) AGAINST TEST STRAINS

Test bacteria	Al_2S_3 nanoparticles	Positive control gentamycin (10 μg)
Bacillus subtilis MTCC 2763	17.04 ± 0.04	20.05 ± 0.08
Escherichia coli MTCC 40	15.10 ± 0.13	22.14 ± 0.15

TABLE-5
EFFECT OF RATE OF DEGRADATION IN SUNLIGHT AND UV LIGHT

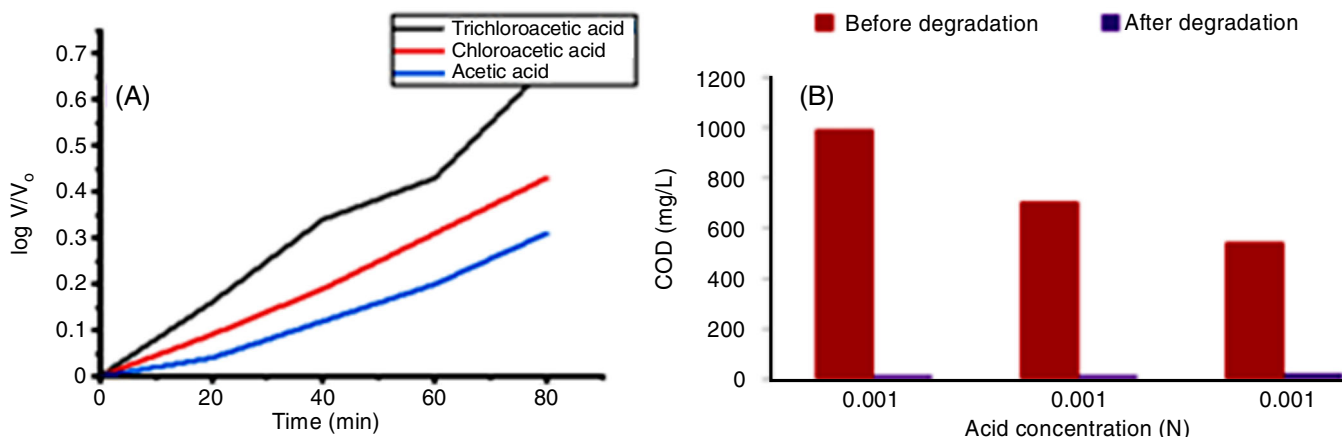| Catalyst 0.02 g	Concentration of carboxylic acid (0.001 N)	Sunlight (10^{-3} k s⁻¹)	Time taken for 95% degradation (min)	UV light (10^{-3} k s⁻¹)	Time taken for 95% degradation (min)
Al_2S_3 nanoparticles	Cl_3CCOOH	0.310	160	2.08	50
	$ClCH_2COOH$	0.207	210	1.89	60
	CH_3COOH	0.149	240	0.99	90

Fig. 11. (A) Effect of concentration of carboxylic acids on the rate of degradation (B) COD values under sunlight

Conclusion

In present study, Al$_2$S$_3$ nanoparticles were synthesized successfully by electrochemical method. To know the activity of synthesized Al$_2$S$_3$ nanoparticles were investigated by the kinetics of photodegradation of carboxylic acids by using volumetric method against NaOH solution. Kinetics of photodegradation of carboxylic acids recommended that the degradation of acids follows first order kinetics. The photodegradation were carried out in UV light and sunlight, the study shows the rate is low in sunlight when compared to UV light. The complete degradation of acid solution was confirmed by COD measurement. The COD values revealed that 96% of acid had been degraded. The synthesized nanoparticles also showed a moderate inactivation of different strains of bacteria.

CONFLICT OF INTEREST

The authors declare that there is no conflict of interests regarding the publication of this article.

REFERENCES

1. Sowbhagya and S. Ananda, *Am. Chem. Sci. J.*, **4**, 616 (2014).
2. G. Doria, J. Conde, B. Veigas, L. Giestas, C. Almeida, M. Assuncao, J. Rosa and P.V. Baptista, *Sensors*, **12**, 1657 (2012);
    https://doi.org/10.3390/s120201657
3. W.P. McConnell, J.P. Novak, L.C. Brousseau, R.R. Fuierer, R.C. Tenent and D.L. Feldheim, *J. Phys. Chem. B*, **104**, 8925 (2000);
    https://doi.org/10.1021/jp000926t
4. M. Kooti and L. Matouri, *Res. Revs: J. Mater. Sci.*, **2**, 37 (2013).
5. A.S. Aldwayyan, F.M. Al-Jekhedab, M. Al-Noaimi, B. Hammouti, T.B. Hadda, M. Suleiman and I. Warad, *Int. J. Electrochem. Sci.*, **8**, 10506 (2013).
6. P. Kulkarni, S.K. Nataraj, R.G. Balakrishna, D.H. Nagaraju and M.V. Reddy, *J. Mater. Chem. A*, **5**, 22040 (2017);
    https://doi.org/10.1039/C7TA07329A
7. M. Shen, C. Ruan, Y. Chen, C. Jiang, K. Ai and L. Lu, *ACS Appl. Mater. Interfaces*, **7**, 1207 (2015);
    https://doi.org/10.1021/am507033x
8. Z. Ma, X. Yuan, Z. Zhang, D. Mei, L. Li, Z.-F. Ma, L. Zhang, J. Yang and J. Zhang, *Sci. Rep.*, **5**, 18199 (2015);
    https://doi.org/10.1038/srep18199
9. X. Meng, Y. Cao, J.A. Libera and J.W. Elam, *Chem. Mater.*, **29**, 19043 (2017);
    https://doi.org/10.1021/nn505480w
10. C.-H. Lai, M.-Y. Lu and L.-J. Chen, *J. Mater. Chem.*, **22**, 19 (2012);
    https://doi.org/10.1039/C1JM13879K
11. J. Cabana, L. Monconduit, D. Larcher and M.R. Palacin, *Adv. Mater.*, **22**, E170 (2010);
    https://doi.org/10.1002/adma.201000717
12. L.J. Lopes, A.C. Estrada, S.Fateixa, M. Ferro and T. Trindade, *Nanomaterials*, **7**, 245 (2017);
    https://doi.org/10.3390/nano7090245
13. T. Trindade and P.J. Thomas, Defining and Using Very Small Crystals, In: Comprehensive Inorganic Chemistry II, Elsevier: Oxford, MS, USA, edn 2, vol. 4, pp. 343-369 (2013).
14. G.H.A. Therese and P.V. Kamath, *Chem. Mater.*, **12**, 1195 (2000);
    https://doi.org/10.1021/cm990447a
15. M. Kristl, S. Gyergyek, N. Srt and I. Ban, *Mater. Manuf. Process.*, **31**, 1608 (2016);
    https://doi.org/10.1080/10426914.2015.1103860
16. A.P. Velmuzhov, M.V. Sukhanov, V.S. Shiyaev, M.F. Churbanov and A.I. Suchov, *Chalcogenide Lett.*, **10**, 443 (2013).
17. V.V. Kulish, D. Koch and S. Manzhos, *Phys. Chem. Chem. Phys.*, **19**, 6076 (2017);
    https://doi.org/10.1039/C6CP08284J
18. X. Sun, P. Bonnick and L.F. Nazar, *ACS Energy Lett.*, **1**, 297 (2016);
    https://doi.org/10.1021/acsenergylett.6b00145
19. P.A. Ajibade and J.Z. Mbese, *Int. J. Polym. Sci.*, **2014**, 752394 (2014);
    https://doi.org/10.1155/2014/752394
20. T.P. Mthethwa, M.J. Moloto, A. deVries and K.P. Matabola, *Mater. Res. Bull.*, **46**, 569 (2011);
    https://doi.org/10.1016/j.materresbull.2010.12.022
21. A. Khan, *J. Nanomater.*, **2012**, 451506 (2012);
    https://doi.org/10.1155/2012/451506
22. Y.-R. Hong, S. Mhin, J. Kwon, W.-S. Han, T. Song and H.S. Han, *R. Soc. Open Sci.*, **5**, 180927 (2018);
    https://doi.org/10.1098/rsos.180927
23. N. Armaroli and V. Balzani, *Angew. Chem. Int. Ed.*, **46**, 52 (2007);
    https://doi.org/10.1002/anie.200602373
24. G. Chaitanya Lakshmi, S. Ananda and C. Somashekar, *Int. J. Adv. Mater. Sci.*, **3**, 221 (2012).
25. K. Byrappa, A.K. Subramani, S. Ananda, K.M.L. Rai, R. Dinesh and M. Yoshimura, *Bull. Mater. Sci.*, **29**, 433 (2006);
    https://doi.org/10.1007/BF02914073
26. S. Kondawar, R. Mahore, A. Dahegaonkar, *Adv. Appl. Sci. Res.*, **2**, 401 (2011).
27. X.Y. Ma, G.X. Lu and B.J. Yang, *Appl. Surf. Sci.*, **187**, 235 (2002);
    https://doi.org/10.1016/S0169-4332(01)00994-1
28. X.R. Ye, C. Daraio, C. Wang, J.B. Talbot and S. Jin, *J. Nanosci. Nanotechnol.*, **6**, 852 (2006);
    https://doi.org/10.1166/jnn.2006.135
29. T.P. Sharma, D. Patidar, N.S. Saxena and K. Sharma, *Indian J. Pure Appl. Phys.*, **44**, 520 (2006).
30. R.S. Ananda, N.M.M. Gowda and K.R. Raksha, *Adv. Nanopart.*, **3**, 133 (2014);
    https://doi.org/10.4236/anp.2014.34018
31. K.R. Raksha and S. Ananda, *J. Appl. Chem.*, **3**, 397 (2014).
32. B. Kraeutler and A.J. Bard, *J. Am. Chem. Soc.*, **100**, 5985 (1978);
    https://doi.org/10.1021/ja00487a001
33. O. Exner, *Collect. Czech. Chem. Commun.*, **29**, 1094 (1964);
    https://doi.org/10.1135/cccc19641094
34. R.D. Gillion, Introduction to Physical Organic Chemistry, Addison Wesley, London, pp. 156-160, p. 168 (1970).
35. O. Exner, eds.: N.B. Chapman and J. Shorter, Correlation Analysis in Chemistry, Plenum Press: London (1978).
36. G. Bott, L.D. Field and S. Sternhell, *J. Am. Chem. Soc.*, **102**, 5618 (1980);
    https://doi.org/10.1021/ja00537a036
37. A.W. Bauer, W.M.M. Kirby, J.C. Sherris and M. Turck, *Am. J. Clin. Pathol.*, **45(4_ts)**, 493 (1966);
    https://doi.org/10.1093/ajcp/45.4_ts.493
38. K.S. Khashan, G.M. Sulaiman, F.A. Abdul Ameer and G. Napolitano, *Pak. J. Pharm. Sci.*, **29**, 541 (2016).